Petroleum Science 20 (2023) 2413–2427

Contents lists available at ScienceDirect

Petroleum Science

journal homepage: www.keaipublishing.com/en/journals/petroleum-science

Original Paper

Failure mechanism and influencing factors of cement sheath integrity under alternating pressure

Kuan-Hai Deng [a, *], Nian-Tao Zhou [a], Yuan-Hua Lin [a, **], Yan-Xian Wu [b], Jie Chen [c], Chang Shu [d], Peng-Fei Xie [a]

[a] State Key Laboratory of Oil and Gas Reservoir Geology and Exploitation (Southwest Petroleum University), Chengdu, Sichuan, 610500, China
[b] Engineering Technology Research Institute, PetroChina Xinjiang Oilfield Company, Karamay, Xinjiang, 834000, China
[c] CNPC Xibu Drilling Engineering Company Limited, Urumqi, Xinjiang, 830000, China
[d] Engineering Technology Research Institute, PetroChina Southwest Oil & Gas Field Company, Chengdu, Sichuan, 610066, China

ARTICLE INFO

Article history:
Received 7 August 2022
Received in revised form
11 January 2023
Accepted 7 March 2023
Available online 8 March 2023

Edited by Jia-Jia Fei

Keywords:
Casing-cement sheath-formation system
Mechanical model
Matching relationship
Cement sheath integrity
Critical range
Mechanical parameters

ABSTRACT

The failure of cement sheath integrity can be easily caused by alternating pressure during large-scale multistage hydraulic fracturing in shale-gas well. An elastic-plastic mechanical model of casing-cement sheath-formation (CSF) system under alternating pressure is established based on the Mohr-Coulomb criterion and thick-walled cylinder theory, and it has been solved by MATLAB programming combining global optimization algorithm with Global Search. The failure mechanism of cement sheath integrity is investigated, by which it can be seen that the formation of interface debonding is mainly related to the plastic strain accumulation, and there is a risk of interface debonding under alternating pressure, once the cement sheath enters plasticity whether in shallow or deep well sections. The matching relationship between the mechanical parameters (elastic modulus and Poisson's ratio) of cement sheath and its integrity failure under alternating pressure in whole well sections is studied, by which it has been found there is a "critical range" in the Poisson's ratio of cement sheath. When the Poisson's ratio is below the "critical range", there is a positive correlation between the yield internal pressure of cement sheath (SYP) and its elastic modulus. However, when the Poisson's ratio is above the "critical range", there is a negative correlation. The elastic modulus of cement sheath is closely related to its Poisson's ratio, and restricts each other. Scientific and reasonable matching between mechanical parameters of cement sheath and CSF system under different working conditions can not only reduce the cost, but also protect the cement sheath integrity.

1. Introduction

In recent years, with the deepening of exploration and development, new oil and gas resources are mainly concentrated in "deep, low permeability, unconventional" fields, such as deep shale gas reservoirs, high temperature and high pressure gas reservoirs and tight gas reservoirs. In the process of deep shale gas exploitation, hydraulic fracturing is a commonly used stimulation method (Shen et al., 2017; Yan et al., 2017). According to the fracturing operation characteristics of shale gas horizontal wells, it can be seen that more than 10 well sections need to be perforated to increase production during the completion of oil and gas wells. Furthermore, the single perforation section is long and the scale of stimulation is large. Fracturing will cause the wellbore to experience continuous and repeated pressure changes, such as alternating pressure rises and falls. In addition, in the late stage of deep shale gas wells production, due to the constantly adjusted/changed production parameters in the wellbore, the pressure will change frequently and periodically. These characteristics can easily lead to the failure of cement sheath integrity in the stimulation section and the upper well section of the oil reservoir, resulting in annular pressure and other problems (Liu et al., 2021), which poses new challenges to ensure the cement sheath integrity under the above-mentioned complex working conditions. Therefore, it is of great

* Corresponding author.
** Corresponding author.
E-mail addresses: dengkuanhai@163.com (K.-H. Deng), yhlin28@163.com (Y.-H. Lin).

https://doi.org/10.1016/j.petsci.2023.03.004

significance to solve the failure of cement sheath integrity and the resulting annular pressure problem for deep shale gas wells in China.

In terms of theoretical analysis, the mechanical model of CSF system under temperature and pressure has been firstly established in 1998, in which the casing, cement sheath and formation were all assumed to be thermos-elasticity (Thiercelin et al., 1998), but the plasticity of cement sheath has not been considered. Mueller et al. (2004) first assumed that the initial state of CSF system was the overburden pressure, and established a CSF system mechanics model to evaluate the sealing performance of cement sheath under different temperatures and pressures. Some researchers have established a series theoretical model of CSF system based on elastic-plastic theory, which could simply calculate the stress-strain and its distribution during loading, whereas these model above could not explain interface debonding (Li et al., 2005a; Yin et al., 2006; Chen and Cai, 2009). Zeng et al. (2019) established a coupled mechanical model to analyze the effects of multi-layer cemented casing, non-uniform formation stress and fracture pressure on the mechanical characteristics of casing and cement during fracturing of shale gas wells. Meng et al. (2021) proposed a coupled mechanical model considering the initial stress state and transient thermos-elastic effects. In addition, some new method are used to study the damage to cement sheath and monitor the integrity of cement-casing system (Zhang et al., 2022a; Li et al., 2022). Zhang et al. (2022b) established a plastic mechanical model of CSF system under asymmetric load based on shakedown theory. The mechanical models established above are mainly aimed at casing damage and body failure of cement sheath, and all focus on the stress-strain and its distribution of CSF system under the certain external loading (Thiercelin et al., 1998; Mueller et al., 2004; Liu et al., 2016; Zeng et al., 2019; Meng et al., 2021). However, there are relatively few studies on the interface debonding under variable casing pressure, especially lacking the mechanical models that quantitatively describe the initiation and development of interface debonding. The formation mechanism of interface debonding under variation casing pressure are successively studied by some researchers (Zhao et al., 2015; Chu et al., 2015; Shen et al., 2017), whereas the formation mechanism of interface debonding under alternating pressure has not been explained theoretically.

In terms of the failure mechanism of cement sheath integrity, since the 1990s, a series of CSF system test devices have been developed based on the similarity principle, and the integrity of CSF system (mechanical integrity and sealing integrity) has been tested and evaluated by domestic and foreign scholars (Goodwin and Crook, 1992; Jackson and Murphey, 1993; Boukhelifa et al., 2005; De Andrade et al., 2016; Therond et al., 2017). In recent years, more and more scholars pay attention to the failure of cement sheath integrity under alternating pressure (De Andrade et al., 2015; Tao, 2018; Guan et al., 2021; Liu R. et al., 2016). Fan et al. (2016) and Lamik et al. (2021) all believe that plastic deformation take place inside the cement sheath under the high stress, as the alternating goes on, the plastic deformation gradually accumulates and the plastic deformation will be converted into residual deformation after unloading. The deformation difference between casing and cement sheath at the interface produces tensile stress. When exceeding the bonding strength at the interface, the interface debonding will occur. Wang et al. (2019) believes that cyclic loading is the main reason for the sealing failure of cement sheath, and the cement sheath interface failure is more likely to occur in the deep layer. Zhou et al. (2019) and Xi et al. (2020a) studied the mechanical properties and integrity of cement sheath under alternating pressure, and both believed that the cumulative plastic deformation increased with the increase of the number of cycles. They all believe that the failure of cement sheath integrity, especially the interface failure, is mainly caused by the accumulation of plastic strain (Fan et al., 2016; Lamik et al., 2021; Zhou et al., 2019). In addition, the retrogression of mechanical properties (permeability and porosity increase, compressive and tensile strength decrease) and the degradation of interfacial bonding strength (shear, axial and radial bonding strength) may aggravates cement sheath integrity failure under alternating load (Lin et al., 2020; Deng et al., 2020). Therefore, it is urgent to prevent cement sheath of generating plastic strain.

In preventive measures on the failures of cement sheath integrity, some cement slurry systems have been developed to improve the cement sheath integrity (Agzamov and Ismagilova, 2019; Contreras et al., 2019; Yang et al., 2021). Li et al. (2005b) and Wang et al. (2008) concluded that the ideal cement sheath should have both high strength and low stiffness. Based on simulation analysis, Bu et al. (2016) obtained that the relationship between the elastic modulus of cement sheath and the stress distribution of cement sheath is a positive correlation, and its Poisson's ratio is negatively correlated with its stress distribution. Zhao et al. (2015), Li et al. (2019), Fan et al. (2019), and Xi et al. (2020b) all proposed that reducing the elastic modulus of cement sheath can improve its long-term sealing capacity. They all believe that the failure of cement sheath integrity can be solved by reducing its elastic modulus, that is, the lower the better. However, the elastic modulus of cement sheath cannot be indefinitely decreased (Liu et al., 2021), that is the lower the elastic modulus, the lower the cement sheath strength (De Andrade and Sangesland, 2016). The cost of obtaining cement sheath with high strength and low stiffness is often high, which obviously does not meet the requirements of cost reduction and efficiency increase. Hence, it is particularly important to study the matching relationship between the mechanical parameters of cement sheath and CSF system in order to obtain the optimal of cement sheath to ensure the cement sheath integrity under different working conditions.

Based on these, one elastic-plastic mechanical analysis model of the CSF system under alternating pressure is established and solved by the MATLAB programming combining global optimization algorithm with Global Search. The failure mechanism of cement sheath integrity under alternating pressure are analyzed, and the matching relationship between the mechanical parameters of cement sheath and the CSF system is established.

2. Elastic-plastic mechanical model of CSF system

The casing, cement sheath and formation are closely connected with each other after cementing, so the thick wall cylinder theory could be used to analyze them. The thick-walled cylinder subjected to internal and external pressure can generally be simplified as a plane strain problem without considering the change of ground stress along the axial direction. The model is shown in Fig. 1, and the three assumptions are made as follow. Firstly, the casing and formation conform to the elastic law, the cement sheath conforms to the elastic-plastic law, and the Mohr-Coulomb yield criterion was selected for yield condition of cement sheath. Secondly, the casing, cement sheath and formation are ideal cylinders with uniform thickness and concentric with each other. Finally, the cement sheath is in complete contact with the formation and casing at casing-cement sheath interface (CS interface) and cement sheath-formation interface (SF interface) without sliding.

2.1. Mechanical model of CSF system during first loading

Mechanical model of CSF system during first loading and unloading of casing pressure has been derived by some scholars (Chu et al., 2015), this paper focuses on the mechanical model of

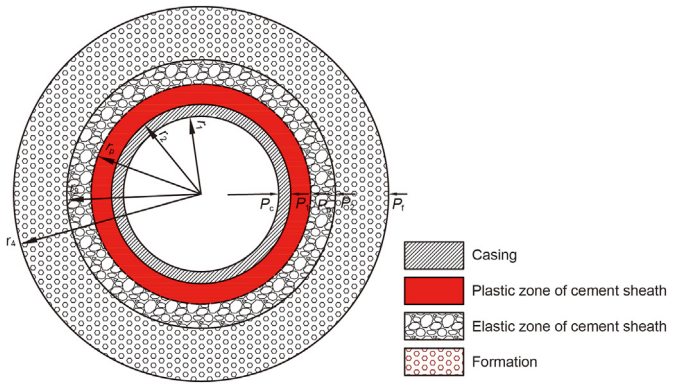

Fig. 1. Mechanical model of CSF system.

CSF system under alternating casing pressure, and the detailed derivation process of formula is shown in Fig. 2.

2.1.1. Casing stress and displacement analysis

The CSF system satisfies boundary condition at the CS interface ($\sigma_{ra} = -P_1$ when $r = r_1$), the stress component and radial displacement of casing could be obtained by adopting the thick-walled cylinder theory (Li et al., 2005a; Chu et al., 2015).

$$\sigma_{ra} = \frac{r_1^2}{r_2^2 - r_1^2}\left(1 - \frac{r_2^2}{r^2}\right)P_c - \frac{r_2^2}{r_2^2 - r_1^2}\left(1 - \frac{r_1^2}{r^2}\right)P_1 \tag{1}$$

$$\sigma_{\theta a} = \frac{r_1^2}{r_2^2 - r_1^2}\left(1 + \frac{r_2^2}{r^2}\right)P_c - \frac{r_2^2}{r_2^2 - r_1^2}\left(1 + \frac{r_1^2}{r^2}\right)P_1 \tag{2}$$

$$u_a = \frac{(1+\mu_1)}{E_1}\frac{(1-2\mu_1)r_1^2 r^2 + r_1^2 r_2^2}{r(r_2^2 - r_1^2)}P_c - \frac{(1+\mu_1)}{E_1}\frac{(1-2\mu_1)r_2^2 r^2 + r_1^2 r_2^2}{r(r_2^2 - r_1^2)}P_1 \tag{3}$$

where σ_{ra} is the radial stress of casing, MPa; $\sigma_{\theta a}$ is the circumferential stress of casing, MPa; μ_1 is the Poisson's ratio of casing; E_1 is the elastic modulus of casing, GPa; r is the radius of the CSF system, mm; r_1 is the inner radius of casing, mm; r_2 is the outer radius of casing, mm; P_c is the inner casing pressure, MPa; P_1 is the radial stress at CS interface, MPa; u_a is the radial displacement of casing, μm.

The radial displacement at outer wall of casing can be obtained by Eq. (4).

$$u_{ao} = \frac{1+\mu_1}{E_1}\frac{2(1-\mu_1)r_1^2 r_2}{r_2^2 - r_1^2}P_c - \frac{1+\mu_1}{E_1}\frac{r_1^2 r_2 + (1-2\mu_1)r_2^3}{r_2^2 - r_1^2}P_1 \tag{4}$$

where u_{ao} is the radial displacement at the outer wall of casing, μm.

2.1.2. Stress and displacement of cement sheath analysis

The yield condition of cement sheath satisfies Mohr-Coulomb yield criterion.

$$\frac{1}{2}A(\sigma_{\theta b} - \sigma_{rb}) + \frac{1}{2}(\sigma_{\theta b} + \sigma_{rb})\sin\varphi - c\cos\varphi = 0 \tag{5}$$

where σ_{rb} is the radial stress of cement sheath, MPa; $\sigma_{\theta b}$ is the circumferential stress of cement sheath, MPa; φ is the internal friction angle of cement sheath, °; c is the cohesion of cement sheath, MPa.

Combining Eq. (5) and Equilibrium equation with boundary conditions at the CS interface ($\sigma_r = -P_1$ when $r = r_2$), the radial and circumferential stress in plastic zone can be given as follow.

$$\begin{cases} \sigma_{rb} = c\cot\varphi\left[1 - \left(1 + \dfrac{P_1}{c\cot\varphi}\right)\left(\dfrac{r}{r_2}\right)^{B-1}\right] \\ \sigma_{\theta b} = c\cot\varphi\left[1 - B\left(1 + \dfrac{P_1}{c\cot\varphi}\right)\left(\dfrac{r}{r_2}\right)^{B-1}\right] \end{cases} \tag{6}$$

where $B = (A\text{-}\sin\varphi)/(A + \sin\varphi)$.

Combining with Eq. (6), under the boundary condition at interface between elastic-plastic zone of cement sheath ($\sigma_{rb} = P_p$ when $r = r_p$), the radial stress at interface between elastic-plastic zone of cement sheath can be obtained by Eq. (7).

$$P_p = c\cot\varphi\left[\left(1 + \frac{P_1}{c\cot\varphi}\right)\left(\frac{r_p}{r_2}\right)^{B-1} - 1\right] \tag{7}$$

where P_p is the radial stress at interface between elastic-plastic zone of cement sheath, MPa; r_p is the radius at interface between elastic-plastic zone of cement sheath, mm.

Ignoring the volume change in the plastic deformation, Eq. (8) can be obtained as follow (Chen and Salip, 2004; Chu et al., 2015).

$$\varepsilon_{rb} + \varepsilon_{\theta b} = \frac{(1+\mu_2)(1-2\mu_2)}{E_2}(\sigma_{rb} + \sigma_{\theta b}) \tag{8}$$

where μ_2 is the Poisson's ratio of cement sheath; E_2 is the elastic modulus of cement sheath, GPa.

The displacements continuity condition at interface between elastic zone and plastic zone of cement sheath can be given as follow.

$$u_{bpo} = u_{bei} \tag{9}$$

where u_{bpo} is the radial displacement at the outer wall in plastic zone of cement sheath, μm; u_{bei} is the radial displacement at the inner wall in elastic zone of cement sheath, μm.

The displacement at inner wall in the elastic zone of cement sheath (u_{bei}) can be obtained by thick-walled cylinder theory (Li et al., 2005a; Chu et al., 2015).

$$u_{bei} = \frac{1+\mu_2}{E_2}\frac{r_p r_3^2 + (1-2\mu_2)r_3^3}{r_3^2 - r_p^2}P_p - \frac{1+\mu_2}{E_2}\frac{2(1-2\mu_2)r_p r_3^2}{r_3^2 - r_p^2}P_2 \tag{10}$$

where r_3 is the outer radius of cement sheath, mm; P_2 is the radial stress at SF interface, MPa.

The general solution of the displacement in the plastic zone of cement sheath can be obtained by combining Eq. (6), Eq. (8) and Geometric equation. The integral constant can be obtained by boundary condition ($u_{bpo} = u_{bei}$ when $r = r_p$). Combining with Eq. (9) and Eq. (10), the displacement at the plastic zone of cement

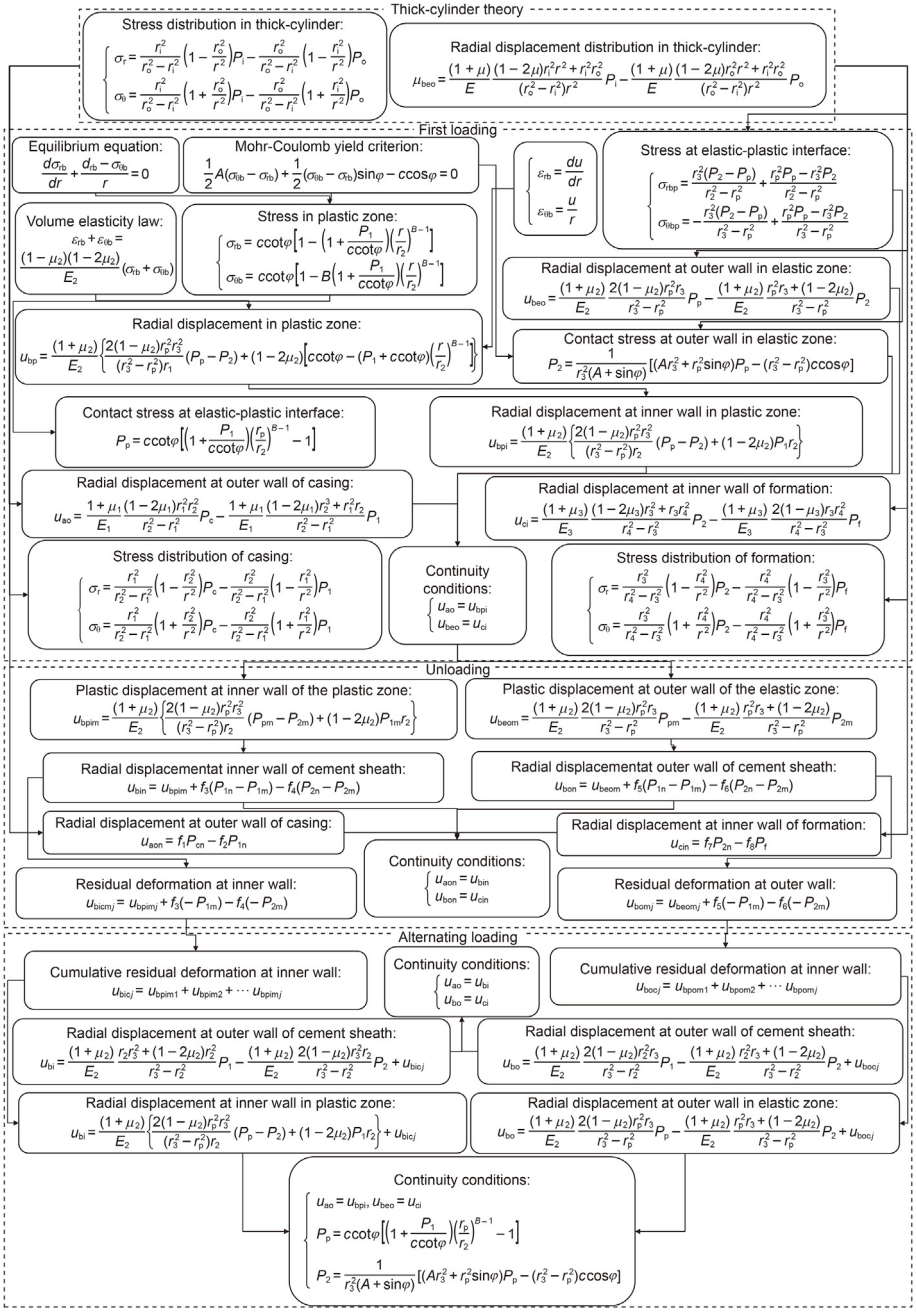

Fig. 2. Formula derivation flow chart.

sheath can be obtained as follow.

where u_{bp} is the radial displacement in plastic zone of cement sheath, μm.

$$u_{bp}=\frac{(1+\mu_2)}{E_2}\left\{\frac{2(1-\mu_2)r_p^2r_3^2}{\left(r_3^2-r_p^2\right)r_1}\left(P_p-P_2\right)+(1-2\mu_2)\left[c\cot\varphi-(P_1+c\cot\varphi)\left(\frac{r}{r_2}\right)^{B-1}\right]r\right\} \tag{11}$$

The radial displacements at inner wall in plastic zone of cement sheath can be obtained through the boundary condition ($u_{bp} = u_{bpi}$ when $r = r_1$).

$$u_{bpi} = \frac{(1+\mu_2)}{E_2}\left[\frac{2(1-\mu_2)r_p^2 r_3^2}{\left(r_3^2 - r_p^2\right)r_2}(P_1 - P_2) - (1-2\mu_2)P_1 r_2\right] \tag{12}$$

where u_{bpi} is the radial displacement at the inner wall in plastic zone of cement sheath, μm.

The principal stress at the interface between elastic zone and plastic zone ($r = r_p$) can be obtained by adopting the thick-walled cylinder theory (Li et al., 2005a; Chu et al., 2015) and the boundary conditions ($\sigma_{rb} = P_p$ when $r = r_p$, σ_{rb}=P_2 when $r = r_2$).

$$\begin{cases} \sigma_{rbp} = \dfrac{r_3^2(P_2 - P_p)}{r_3^2 - r_p^2} + \dfrac{r_p^2 P_p - r_3^2 P_2}{r_3^2 - r_p^2} \\ \sigma_{\theta bp} = -\dfrac{r_3^2(P_2 - P_p)}{r_3^2 - r_p^2} + \dfrac{r_p^2 P_p - r_3^2 P_2}{r_3^2 - r_p^2} \end{cases} \tag{13}$$

where σ_{rbp} is the radial stress at interface between elastic zone and plastic zone of cement sheath, MPa; $\sigma_{\theta bp}$ is the circumferential stress at interface between elastic zone and plastic zone of cement sheath, MPa.

The radial stress P_2 at SF interface can be obtained by combining Eq. (5) and Eq. (13).

$$P_2 = \frac{1}{r_3^2(A + \sin\varphi)}\left[\left(Ar_3^2 + r_p^2\sin\varphi\right)P_p - \left(r_3^2 - r_p^2\right)c\cos\varphi\right] \tag{14}$$

The radial displacement at inner wall in elastic zone of cement sheath can be obtained by boundary condition ($u_{be} = u_{beo}$ when $r = r_2$).

$$u_{beo} = \frac{1+\mu_2}{E_2}\frac{2(1-\mu_2)r_p^2 r_3}{r_3^2 - r_p^2}P_p - \frac{1+\mu_2}{E_2}\frac{r_p^2 r_3 + (1-2\mu_2)r_3{}^3}{r_2^2 - r_p^2}P_2 \tag{15}$$

where u_{beo} is the radial displacement at the outer wall in elastic zone of cement sheath, μm.

2.1.3. Formation displacement analysis

Similarly, the radial displacement at inner wall of formation can be obtained by adopting the thick-walled cylinder theory (Li et al., 2005a; Chu et al., 2015).

$$u_{ci} = \frac{1+\mu_3}{E_3}\frac{r_3 r_4^2 + (1-2\mu_3)r_3^3}{r_4^2 - r_3^2}P_2 - \frac{1+\mu_3}{E_3}\frac{2(1-\mu_3)r_3 r_4^2}{r_4^2 - r_3^2}P_f \tag{16}$$

where μ_3 is the Poisson's ratio of formation; E_3 is the elastic modulus of formation, GPa; r_4 is the outer radius of formation, mm; P_f is the formation stress, MPa; u_{ci} is the radial displacement at the inner wall of formation, μm.

2.1.4. Displacement continuity conditions of CSF system

It is considered by adopting boundary conditions of ideal complete contact during the loading process. Hence, the radial displacement boundary conditions at the CS interface and SF interface can be obtained by Eq. (17).

$$\begin{cases} u_{ao} = u_{bpi} \\ u_{beo} = u_{ci} \end{cases} \tag{17}$$

Therefore, the mechanical model of CSF system during loading can be obtained by Eq. (18).

$$\begin{cases} u_{ao} = u_{bpi}\ ,\ u_{beo} = u_{ci} \\ P_p = c\cot\varphi\left[\left(1 + \dfrac{P_1}{c\cot\varphi}\right)\left(\dfrac{r_p}{r_2}\right)^{B-1} - 1\right] \\ P_2 = \dfrac{1}{r_3^2(A+\sin\varphi)}\left[\left(Ar_3^2 + r_p^2\sin\varphi\right)P_p - \left(r_3^2 - r_p^2\right)c\cos\varphi\right] \end{cases} \tag{18}$$

Under the condition of knowing the casing internal pressure P_c and formation stress P_f, the four unknowns (P_1, P_p, P_2, r_p) can be obtained by solving the four element equations, the stress and displacement of the CSF system during the loading stage can be calculated.

2.2. The yield internal pressure of cement sheath during first loading

In the process of casing pressure loading, the cement sheath gradually transitions from the elastic state to the plastic state. The inner wall of cement sheath first yields and enters the plastic state. The state that the cement sheath just enters the plastic state is defined as the yield failure of cement sheath, and this casing pressure is defined as SYP, which satisfies Eq. (19).

$$\begin{cases} r_p = r_2\ ,\quad P_p = P_1 \\ P_2 = \dfrac{1}{r_3^2(A+\sin\varphi)}\left[\left(Ar_3^2 + r_2^2\sin\varphi\right)P_1 - \left(r_3^2 - r_2^2\right)c\cos\varphi\right] \end{cases} \tag{19}$$

Then the displacement continuity condition can be obtained as follows.

$$\begin{cases} u_{ao} = u_{bei}\ ,\quad u_{beo} = u_{ci} \\ P_2 = \dfrac{1}{r_3^2(A+\sin\varphi)}\left[\left(Ar_3^2 + r_2^2\sin\varphi\right)P_1 - \left(r_3^2 - r_2^2\right)c\cos\varphi\right] \end{cases} \tag{20}$$

This equation system is a three-element equation system about unknown P_c, P_1, P_2. The SYP can be solved by this equation under formation pressure P_f.

2.3. Interface stress of cement sheath during unloading

The relationship between stress and strain of plastic materials is linear when unloading, and the slope is basically the same as that of the elastic stage when loading (Chen and Salip, 2004). Hence, this paper assumes that the casing, cement sheath, and formation are all in an elastically stage during unloading process (Chu et al., 2015), and the combined stress and strain change due to the pressure reduction in the casing can be obtained by the elastic mechanic method. Based on the elastic-plastic theory, stress state and deformation coordination theory of the CSF system, it can be learned that during the unloading process of the CSF system after loading, plastic deformation takes place inside the cement sheath, and the interface uncoordinated deformation will produce the phenomenon of “interface stress inversion”, which means when unloading begins, the radial compressive stress at the interface of cement sheath gradually decreases, and when unloading reaches a certain degree, the radial compressive stress at the interface appears a critical phenomenon-the radial compressive stress is zero. Then, with the unloading continues, the radial compressive stress

turns into radial tensile stress, and the radial tensile stress increases with the increase of unloading strength, while the elastic deformation of casing can be completely recovered, resulting in incompatible deformation of the CS interface or SF interface. When the radial tensile stress exceeds the bonding strength of the interface, the cement sheath separates from the casing or formation, creating interface debonding and destroying the cement sheath integrity (Xu et al., 2014; Chen, 2017).

When the casing pressure rises to P_{cm} for the first time, the parameters such as the pressure at outer wall of casing (P_{1m}) and the pressure at inner wall of formation (P_{2m}) can be obtained by the CSF system model. After that, the casing pressure is unloaded to P_{cn}, and the corresponding pressure at outer wall of casing (P_{1n}) and the pressure at inner wall of formation (P_{2n}) need to be re-solved.

The casing is an always elastomer during the loading and unloading. The radial displacement at outer wall can be obtained by adopting the thick-walled cylinder theory.

$$u_{aon}=\frac{1+\mu_1}{E_1}\frac{2(1-\mu_1)r_1^2r_2}{r_2^2-r_1^2}P_{cn}-\frac{1+\mu_1}{E_1}\frac{r_1^2r_2+(1-2\mu_1)r_2^3}{r_2^2-r_1^2}P_{1n} \tag{21}$$

where P_{cn} is the casing pressure after unloading, MPa; P_{1n} is the radial stress at CS interface during unloading, MPa; u_{aon} is the radial displacement at the outer wall of casing after unloading, μm.

Similarly, the displacement at inner wall of formation can be given as follows.

$$u_{cin}=\frac{1+\mu_3}{E_3}\frac{r_3r_4^2+(1-2\mu_3)r_3^3}{r_4^2-r_3^2}P_{2n}-\frac{1+\mu_3}{E_3}\frac{2(1-\mu_3)r_3r_4^2}{r_4^2-r_3^2}P_f \tag{22}$$

where u_{cin} is the radial displacement at the inner wall of formation after unloading, μm; P_{2n} is the radial stress at SF interface during unloading, MPa.

During the unloading process, the casing pressure decreased from P_{cm} to P_{cn}, accordingly, the change value of radial stress at CS interface is P_{1n}–P_{1m}, and the change value of radial stress at SF interface is P_{2n}–P_{2m}. Base on the elastic unloading theory, the variation of displacement (u_{bin}) is determined by the plastic displacement at inner wall of the plastic zone during loading (u_{bpim}) and the change of the pressure acting on the cement sheath during unloading, which can be given as follows.

$$u_{bin}=u_{bpim}+\frac{1+\mu_2}{E_2}\frac{r_2r_3^2+(1-2\mu_2)r_2^3}{r_3^2-r_2^2}(P_{1n}-P_{1m})-\frac{1+\mu_2}{E_2}\frac{2(1-2\mu_2)r_2r_3^2}{r_3^2-r_2^2}(P_{2n}-P_{2m}) \tag{23}$$

where u_{bin} is the radial displacement at the inner wall of cement sheath after unloading, μm; u_{bpim} is the radial displacement at the inner wall in plastic zone of cement sheath during loading, μm; P_{1m} is the radial stress at CS interface under max casing pressure, MPa; P_{2m} is the radial stress at SF interface under max casing pressure, MPa.

Similarly, the displacement at outer wall of cement sheath after unloading can be given as follows.

$$u_{bon}=u_{beom}+\frac{1+\mu_2}{E_2}\frac{2(1-\mu_2)r_2^2r_3}{r_3^2-r_2^2}(P_{1n}-P_{1m})-\frac{1+\mu_2}{E_2}\frac{r_2r_3^2+(1-2\mu_2)r_3^3}{r_3^2-r_2^2}(P_{2n}-P_{2m}) \tag{24}$$

where u_{bon} is the radial displacement at the outer wall of cement sheath after unloading, μm; u_{beom} is the radial displacement at the outer wall in elastic zone of cement sheath during loading, μm.

Before the formation of micro-annulus at interface, the bonding strength of CS interface and SF interface are still greater than tensile stress at both interfaces when the casing pressure decreases to P_{cn}. Hence, the continuous conditions can be still applicable to the CSF system.

$$\begin{cases} u_{aon}=u_{bin} \\ u_{bon}=u_{cin} \end{cases} \tag{25}$$

By solving Eq. (25), the P_{1n} and P_{2n} can be obtained.

2.4. Mechanical model of CSF system under alternating pressure

After the casing pressure loading, the cement sheath will produce plastic deformation and residual deformation after unloading. During the next casing pressure loading and unloading, the residual deformation will be calculated into the continuity equation, and the value of the residual deformation is the superposition of the residual deformation caused by the previous casing pressure loading and unloading.

The casing and formation are always in an elastically stage under alternating pressure, which means no residual deformation for the casing and formation. Hence, the radial displacement at outer wall of casing and inner wall of formation after the multiple loading and unloading (1, 2, 3 … j) of casing pressure can still be given by Eq. (3) and Eq. (16).

After the multiple loading and unloading (1, 2, 3 … j–1) of casing pressure, in the elastic stage of cement sheath, the radial displacement at inner wall of cement sheath is determined by the radial displacement generated during the next loading of casing pressure (j st) and the cumulative residual deformation change at inner wall of cement sheath (u_{bicj}) during previous loading and unloading (1, 2, 3 … j–1) of casing pressure.

$$u_{bi}=\frac{1+\mu_2}{E_2}\frac{r_2r_3^2+(1-2\mu_2)r_2^3}{r_3^2-r_2^2}P_1-\frac{1+\mu_2}{E_2}\frac{2(1-2\mu_2)r_2r_3^2}{r_3^2-r_2^2}P_2+u_{bicj} \tag{26}$$

where,

$$u_{bicj}=u_{bim1}+u_{bim2}+\cdots+u_{bimj-1}$$

Here u_{bicj} is the cumulative residual deformation at the inner wall of cement sheath after the j–1 st casing pressure cycle, μm; u_{bimj} is the residual deformation at the inner wall of cement sheath under j st casing pressure unloading, μm.

Similarly, after the multiple loading and unloading (1, 2, 3 … j–1) of casing pressure, in the elastic stage of cement sheath, the radial displacement at outer wall of cement sheath during the next loading of casing pressure (j st) can be given by Eq. (27).

$$u_{bo}=\frac{1+\mu_2}{E_2}\frac{2(1-\mu_2)r_2^2r_3}{r_3^2-r_2^2}P_1-\frac{1+\mu_2}{E_2}\frac{r_2r_3^2+(1-2\mu_2)r_3^3}{r_3^2-r_2^2}P_2+u_{bocj} \tag{27}$$

where,

$$u_{bocj}=u_{bom1}+u_{bom2}+\cdots+u_{bomj-1}$$

Here u_{bocj} is the cumulative residual deformation at the outer wall of cement sheath after the $j-1$st casing pressure cycle, μm; u_{bomj} is the residual deformation at the outer wall of cement sheath under j st casing pressure unloading, μm.

After the multiple loading and unloading (1, 2, 3 … $j-1$), in elastic stage of cement sheath, the displacement continuity equation during the next loading of casing pressure (j st) can be given by Eq. (28).

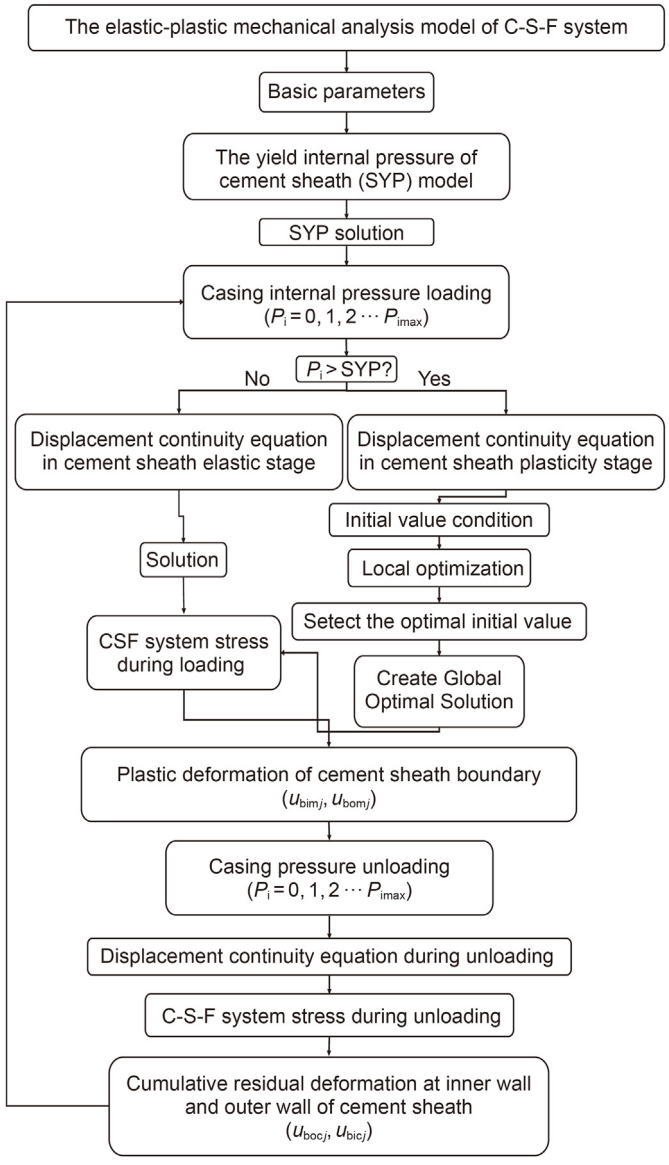

Fig. 3. Solution process for the mechanical model of CSF system.

$$\begin{cases} u_{ao}=u_{bi} \\ u_{bo}=u_{ci} \end{cases} \tag{28}$$

With the increase of casing pressure, the cement sheath gradually transits from elasticity to plasticity. The derivation equation of stress and strain in the plastic stage during the j st casing loading process refers to 1.1.2, therefore, after the multiple loading and unloading (1, 2, 3 … $j-1$), in the plastic stage of cement sheath, the radial displacement at inner wall of cement sheath during the loading of casing pressure at this time (j st) can be given by Eq. (29).

$$u_{bpi}=\frac{(1+\mu_2)}{E_2}\left[\frac{2(1-\mu_2)r_p^2r_3^2}{\left(r_3^2-r_p^2\right)r_2}(P_1-P_2)-(1-2\mu_2)P_1r_2\right]+u_{bicj} \tag{29}$$

Similarly, after the multiple loading and unloading (1, 2, 3 … $j-1$), in the plastic stage of cement sheath, the radial displacement at outer wall of cement sheath during the loading of casing pressure at this time (j st) can be given by Eq. (30).

$$u_{beo}=\frac{1+\mu_2}{E_2}\frac{2(1-\mu_2)r_p^2r_3}{r_3^2-r_p^2}P_p-\frac{1+\mu_2}{E_2}\frac{r_p^2r_3+(1-2\mu_2)r_3{}^3}{r_3^2-r_p^2}P_2+u_{bocj} \tag{30}$$

Hence, after the multiple loading and unloading (1, 2, 3 … $j-1$), in the plastic stage of cement sheath, the displacement continuity equation during the loading of casing pressure at this time (j st) can be given by Eq. (31).

$$\begin{cases} u_{ao}=u_{bpi} \\ u_{beo}=u_{ci} \end{cases} \tag{31}$$

By solving the above model, the stress and strain of CSF system under alternating pressure can be obtained. In this paper the global optimal algorithm Global Search in MATLAB is used to solve the unknown parameters, and the solution process of mechanical model of CSF system in this paper is shown in Fig. 3.

3. Study on the matching relationship between the mechanical parameters of cement sheath and CSF system

3.1. Study on the matching relationship between the cement sheath and the casing

Under high casing pressure, the casing is subjected to large circumferential stress and prone to circumferential damage. Therefore, based on the wellbore structure in reference (Chu et al.,

Table 1
CSF system basic data sheet.

Name of parameter	Value
Inner radius of casing r_1	54.3 mm
Outer radius of casing r_2	63.5 mm
Inner radius of formation r_3	77.39 mm
Outer radius of formation r_4	386.95 mm
Elastic modulus of casing E_1	210 GPa
Poisson's ratio of casing μ_1	0.30
Elastic modulus of cement sheath E_2	5 GPã15 GPa
Poisson's ratio of cement sheath μ_2	0.10–0.30
Elastic modulus of formation E_3	22 GPa
Poisson's ratio of formation μ_3	0.30
Casing pressure P_c	40–70 MPa
Formation stress P_f	0–40 MPa

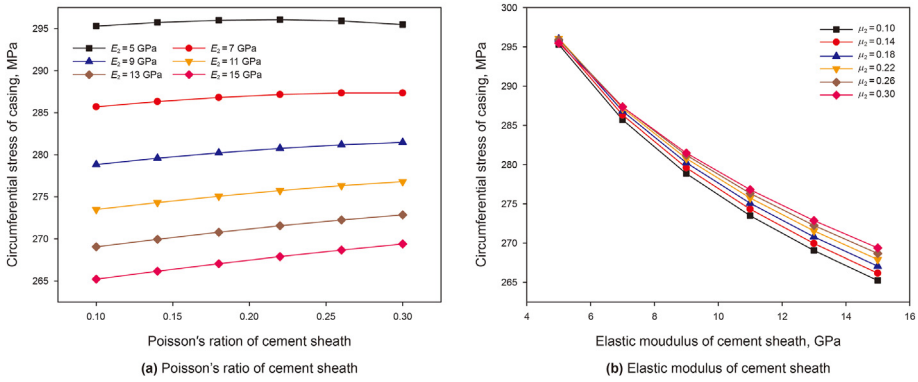

Fig. 4. Relationship between mechanical parameters of cement sheath and the casing circumferential stress (P_c = 70 MPa, P_f = 0 MPa).

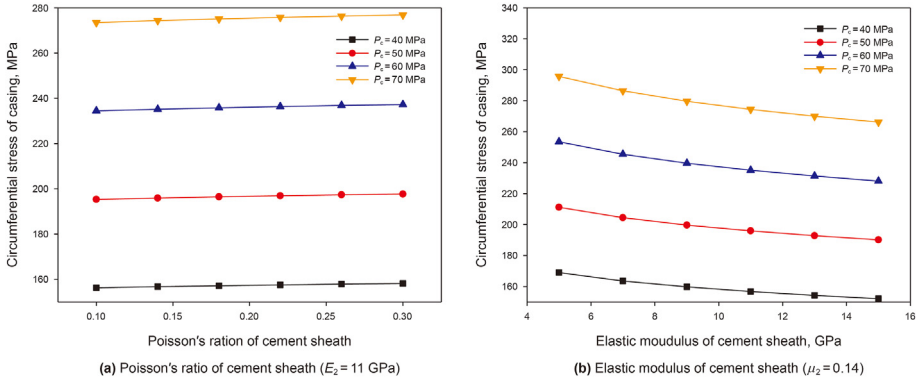

Fig. 5. Casing circumferential stress under different casing pressure.

2015), the matching relationship between the mechanical parameters of cement sheath and the casing circumferential stress is studied. The basic data are shown in Table 1.

The relationship between the casing circumferential stress and the mechanical parameters of cement sheath are shown in Figs. 4 and 5. As is shown in Fig. 4, the cement sheath with low Poisson's ratio and high elastic modulus has a protective effect on casing, but under different elastic modulus conditions, the overall change trend of casing circumferential stress with the Poisson's ratio of cement sheath is slow, indicating that the casing circumferential stress is less sensitive to Poisson's ratio than elastic modulus of cement sheath. Simultaneously, the curves are almost parallel under different casing pressure as shown in Fig. 5, which indicates that the sensitivity of casing circumferential stress to mechanical parameters of cement sheath is not affected by the change of casing pressure.

3.2. Study on the failure of cement sheath integrity during alternating pressure

The failure modes of downhole cement sheath can be divided into two categories, the body failure of cement sheath and interface debonding. Body failure of cement sheath includes yield failure, tensile failure and shear failure. Interface debonding includes CS interface debonding and SF interface debonding (Du, 2016).

During the loading process of casing pressure, the cement sheath is prone to yield failure and tensile failure. With the increase of casing pressure, the cement sheath gradually transits from the elastic state to the plastic state. Firstly, the inner wall of cement sheath commences yield failure and enters the plastic state, then as the loading continues, the plastic range gradually expands to the outer wall of cement sheath until the entire cement sheath enters a complete yield state (Zhang et al., 2017). At the same time, since the tensile strength of cement sheath is far lower than its compressive strength (Liu et al., 2018), while the tensile stress of cement sheath is larger than the tensile strength, it will cause tensile failure, and the cement sheath will produce tensile crack failure (Guo et al., 2018). During casing pressure unloading, the plastic strain is generated due to the cement sheath entering plasticity, and residual strain is generated after completely unloading, which results in uncoordinated deformation at interface. The interface debonding will occur when the radial tensile stress at interface exceeds the bonding strength (Chu et al., 2015). On above basis, the matching relationship between the mechanical parameters of cement sheath and the failure of cement sheath integrity is studied.

3.2.1. Study on yield failure of cement sheath during loading

During the loading of casing pressure, when the inner wall of cement sheath just enters the yield, it is defined as the yield failure of cement sheath, and the casing pressure is defined as SYP. At present, most scholars' research shows that the micro-annular at interface (CS interface or SF interface) is mainly caused by the plastic strain of cement sheath and the accumulation of residual strain during unloading (Liu et al., 2016; Shen et al., 2017; Zeng et al., 2019). Therefore, the SYP should be maximized to avoid or delay the cement sheath generating plastic strain. Based on these, the relationship between the SYP and the mechanical parameters of cement sheath is studied. Zhou's research shows that the yield failure of cement sheath mainly occurs in the deep layer (Zhou et al., 2019), so the formation stress is 40 MPa (P_f = 40 MPa), and

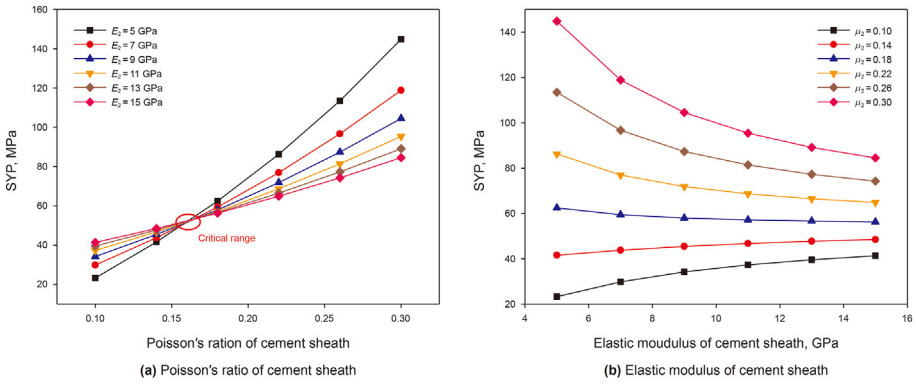

Fig. 6. Relationship between the mechanical parameters of Cement sheath and SYP ($P_f = 40$ MPa).

other basic data is shown in Table 1, and the results are shown in Fig. 6.

It can be known from Fig. 6(a) that under different elastic modulus of cement sheath, the SYP increases gradually with the increase of Poisson's ratio, but sensitivity of SYP to Poisson's ratio of cement sheath decreases with the increase of elastic modulus. At the same time, since the intersections of all curves are about 0.16, the elastic modulus of cement sheath has little effect on the SYP when its Poisson's ratio is about 0.16.

According to Fig. 6(b), when the Poisson's ratio of cement sheath is 0.10–0.16 ($\mu_2 = 0.10–0.16$), the SYP increases with the increase of elastic modulus and finally tends to be stable. When the Poisson's ratio of cement sheath is 0.16 ($\mu_2 = 0.16$), the SYP hardly changes with the increase of elastic modulus. While, when the Poisson's ratio of cement sheath is 0.18–0.30 ($\mu_2 = 0.16–0.30$), the abnormality occurs, with the increase of its elastic modulus, the SYP decreases and finally tends to keep in a steady level.

Hence, it can be concluded that there is a “critical range” in the Poisson's ratio of cement sheath. When the Poisson's ratio is higher than the “critical range”, the SYP decreases with the increase of its elastic modulus, at this time, reducing the elastic modulus can effectively increase the SYP. When the Poisson's ratio of cement sheath is lower than the “critical range”, the SYP increases with the increase of elastic modulus, at this time, increasing the elastic modulus can increase the SYP. When the Poisson's ratio of cement sheath is near the “critical range”, the SYP has little change with elastic modulus, at this time, changing the elastic modulus has little effect on the SYP.

Comprehensively, the cement sheath integrity is closely related to the mechanical parameters of cement sheath. They affect and interact with each other. Reasonable matching can significantly improve the cement sheath integrity.

3.2.2. Study on tensile failure of cement sheath during loading

Tensile failure of cement sheath is mainly affected by the circumferential tensile stress of cement sheath, and it occurs when the circumferential tensile stress of cement sheath is greater than its tensile strength (Guo et al., 2018). Under casing pressure, the circumferential tensile stress at inner wall of cement sheath is the largest, and the tensile failure occurs firstly (Bu et al., 2016). Zhou and Zeng et al. shows that the tensile failure mainly occurs in the fracturing process of shallow formations (Zhou et al., 2019; Zeng et al., 2019), the formation stress is 0 MPa ($P_f = 0$ MPa), and the max casing pressure is loaded to 70 MPa ($P_c = 70$ MPa), other basic data is shown in Table 1. The relationship between the circumferential stress of cement sheath and the mechanical parameters of cement sheath are shown in Figs. 7 and 8.

It can be seen from Fig. 7 that the circumferential stress of cement sheath is more sensitive to the elastic modulus of cement sheath than the Poisson's ratio, and the cement sheath with low elastic modulus and high Poisson's ratio is conducive to reduce the cement sheath circumferential stress of cement sheath. When the elastic modulus of cement sheath is 7–15 GPa ($E_2 = 7–15$ GPa), the cement sheath has already entered plasticity under the casing pressure of 70 MPa ($P_c = 70$ MPa). At this time, the circumferential stress of cement sheath decreases with the increase of its Poisson's ratio, but the curve is almost a straight line which indicates it's less sensitive to the Poisson's ratio of cement sheath. However, when the elastic modulus of cement sheath is 5 GPa ($E_2 = 5$ GPa), the circumferential stress of cement sheath decreases significantly

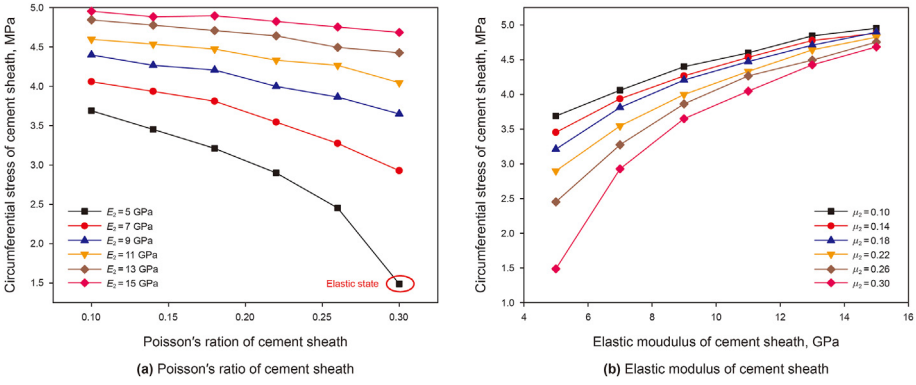

Fig. 7. Relationship between mechanical parameters of cement sheath and cement sheath circumferential stress ($P_c = 70$ MPa, $P_f = 0$ MPa).

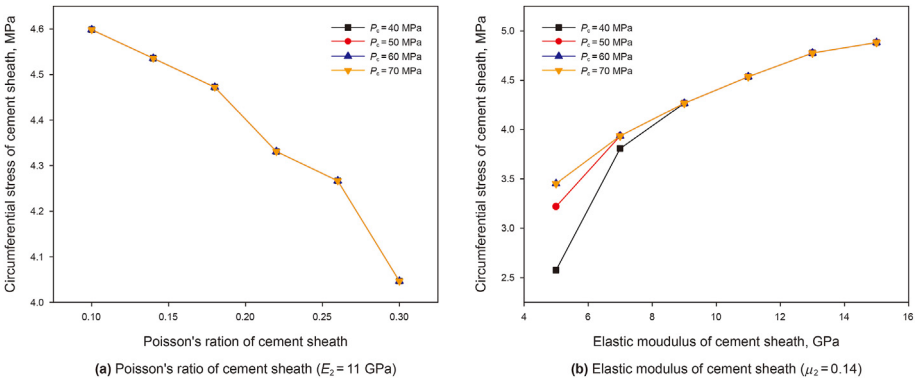

(a) Poisson's ratio of cement sheath (E_2 = 11 GPa) **(b)** Elastic modulus of cement sheath (μ_2 = 0.14)

Fig. 8. Circumferential stress of cement sheath under different casing pressures.

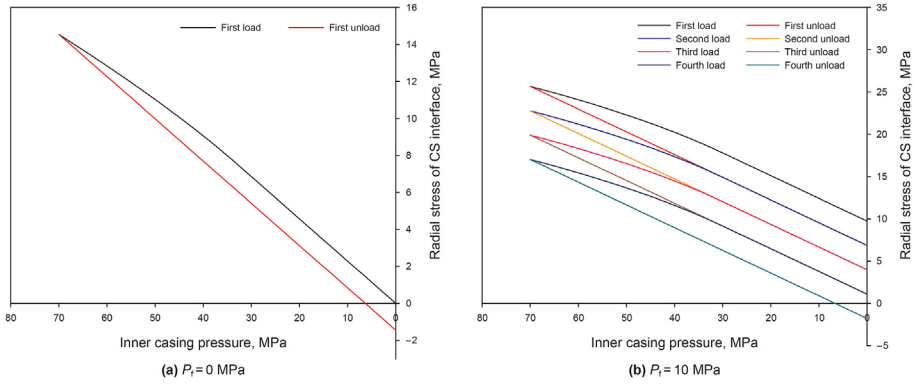

(a) P_f = 0 MPa **(b)** P_f = 10 MPa

Fig. 9. The radial stress of CS interface during loading and unloading.

with the increase of the Poisson's ratio of cement sheath, since it has not yet entered the plastic stage and is in an elastic state, and the circumferential stress of cement sheath is more highly sensitive to the Poisson's ratio of cement sheath at this time. During the loading process, the maximum circumferential tensile stress at inner wall of cement sheath is the circumferential stress when the cement sheath just enters plasticity, and then gradually decreases with the increase of casing pressure, finally the circumferential tensile stress will be converted into circumferential compressive stress (Shen et al., 2017). Therefore, when the casing pressure is 40–70 MPa (P_c = 40–70 MPa), the maximum circumferential stress of cement sheath coincides, which could be verified by Fig. 8.

3.2.3. Study on interface debonding during unloading

In the shallow well section, the formation stress of CSF system is 0 MPa (P_f = 0 MPa). When the casing pressure is large, the cement sheath will deform plastically, and residual strain will be generated during unloading, and then the interface (CS interface or SF interface) will gradually change from a compression state to a tension state. This phenomenon is called "interface stress reversal", which can be shown in Fig. 9(a). However, the casing elastic deformation can be completely recovered, so the outer wall of casing and the inner wall of cement sheath are incompatible deformation. When the radial tensile stress exceeds the bond strength of interface, interface debonding will occur. With the increase of well depth, the formation stress gradually increases (P_f > 0 MPa). After the first

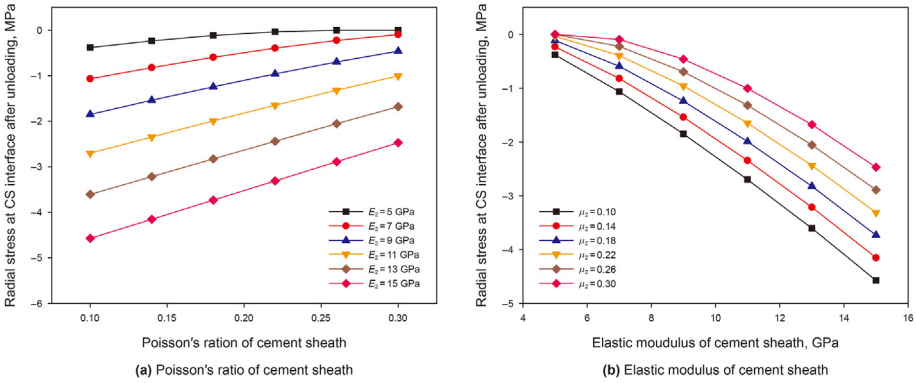

(a) Poisson's ratio of cement sheath **(b)** Elastic modulus of cement sheath

Fig. 10. Relationship between the mechanical parameters of cement sheath and radial stress at CS interface (P_c = 70 MPa, P_f = 0 MPa).

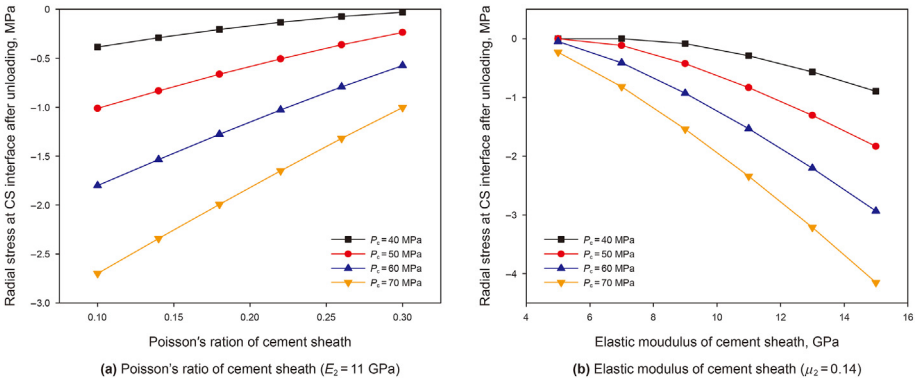

Fig. 11. Radial stress of the CS interface under different casing pressures.

loading and unloading of casing pressure, the interface does not directly experience tension, even if the cement sheath generates plastic strain. However, the residual strain accumulation will still reduce the radial stress at interface after unloading. After multiple loading and unloading of casing, the interface will still take place "interface stress reversal", as shown in Fig. 9(b). When the radial stress at interface exceeds the bonding strength of interface, interface debonding will equally occur at this time. This conclusion can also be proved by the experimental research results of Liu, Zeng and other scholars (Liu et al., 2016; Zeng et al., 2019). Hence, whether in shallow or deep well sections, once the cement sheath enters plasticity, there is a risk of interface debonding under alternating pressure.

Under the high differential pressure and high pump pressure, the cement sheath enters plasticity, resulting in the risk of interface debonding during pressure unloading. At this time, how to reduce the risk of interface debonding by adjusting the mechanical parameters of cement sheath. Based on this, this paper studies the most dangerous point of the interface debonding ($P_f = 0$ MPa), and other basic data is shown in Table 1. The relationship between the tensile stress of the CS interface and the mechanical parameters of cement sheath is studied, and the results are shown in Figs. 10 and 11.

It can be seen from Fig. 10 that both high Poisson's ratio and low elastic modulus of cement sheath can reduce the radial tensile stress at CS interface. Generally speaking, comparing with the Poisson's ratio of cement sheath, the radial tensile stress at CS interface is more sensitive to its elastic modulus. At the same time, it can be seen from Fig. 11 that when the casing pressure is large, the radial tensile stress at CS interface is more sensitive to the mechanical parameters of cement sheath. The higher casing pressure, the higher radial tensile stress at CS interface after unloading, and the greater risk of interface debonding.

In conclusion, the relationship between maximum casing pressure and mechanical parameters of cement sheath should be reasonable matched to avoid the micro-annulus of CSF system.

3.3. Study on the matching relationship between the cement sheath and formation

As shown in Fig. 6, there is a "critical range" for the Poisson's ratio of cement sheath. Therefore, in order to better study the matching relationship between the formation and the cement sheath, the formation stress was selected as 0, 10, 20, 30 MPa (P_f = 0–30 MPa), and combining with 3.2.1, the matching relationship between the mechanical parameters of cement sheath and the SYP under different formation stress conditions is studied and other data are consistent with Table 1. The results are shown in Figs. 12–16.

It can be known from Fig. 12 that when the formation stress is 0 MPa ($P_f = 0$ MPa), the "critical range" is non-existent. Therefore, the SYP increases with the increase of the Poisson's ratio and decreases with the increase of its elastic modulus. When the elastic modulus of cement sheath is from 5 to 15GPa, the sensitivity of SYP to the Poisson's ratio decreases accordingly. It can be known from Figs. 13–15 and Fig. 6, as the formation stress gradually increases from 0 to 10, 20, 30 and 40 MPa, the "critical range" also increases from non-existent to near 0, 0.04, 0.13 and 0.16. It can be seen that the "critical range" of the Poisson's ratio is mainly affected by the formation stress, and increases with the increase of the formation

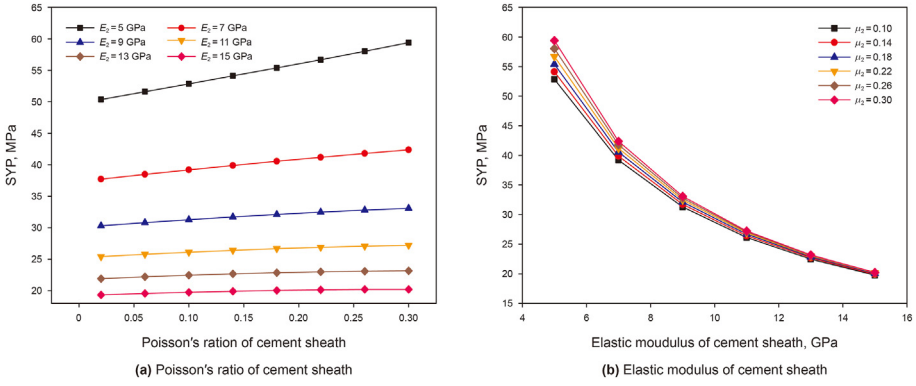

Fig. 12. Relationship between mechanical parameters of cement sheath and the SYP ($P_f = 0$ MPa).

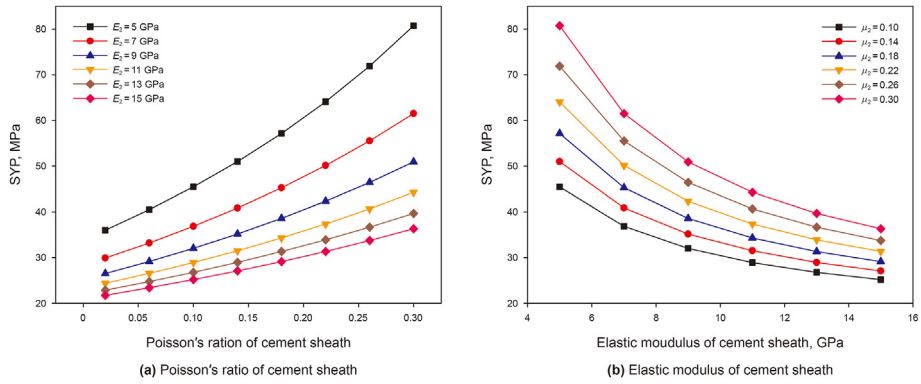

Fig. 13. Relationship between mechanical parameters of cement sheath and the SYP (P_f = 10 MPa).

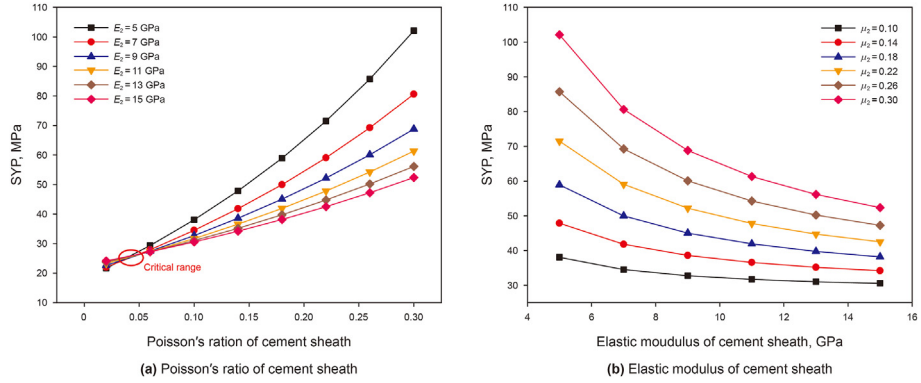

Fig. 14. Relationship between mechanical parameters of cement sheath and the SYP (P_f = 20 MPa).

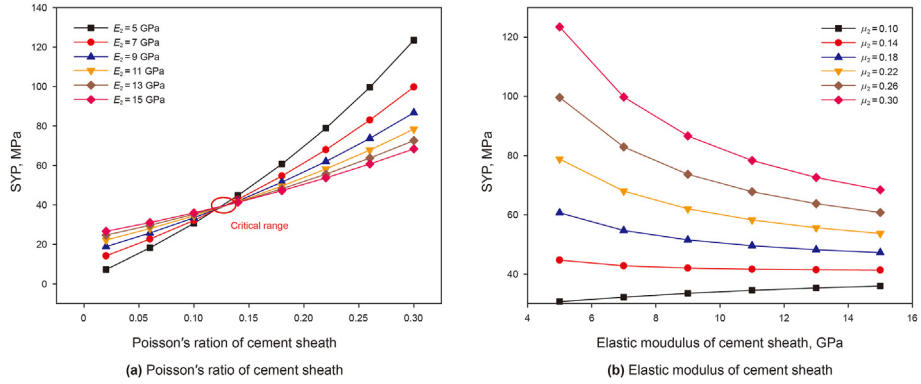

Fig. 15. Relationship between mechanical parameters of cement sheath and the SYP (P_f = 30 MPa).

stress.

Hence, it can be known from Fig. 16, the relationship between the SYP and the elastic modulus of cement sheath is different under different formation stress. When the formation stress is low (P_f = 0–30 MPa), since the Poisson's ratio of cement sheath is above the "critical range", with the increase of its elastic modulus, the SYP increases. As the formation stress gradually increases, the "critical range" of the Poisson's ratio increases accordingly. When the formation stress is 40 MPa (P_f = 40 MPa), the "critical range" of the Poisson's ratio increases to more than 0.14. At this time, the SYP increases with the increase of its elastic modulus.

Based on the above analysis, with the increase of the well depth, the formation stress increases, resulting in different "critical ranges" of Poisson's ratio. Hence, the relationship between the mechanical parameters of cement sheath and the formation stress should be reasonable matched to improve the SYP.

4. Case of matching mechanical parameters of cement sheath with CSF system

Based on the data in Table 1, under different casing pressures, the mechanical parameters of cement sheathe is matched. Since the yield strength of casing is mostly around 850 MPa, under the working conditions of this paper, even if the casing pressure is as high as 70 MPa, the maximum circumferential stress of casing is just 370 MPa, and there is no casing failure, so the casing failure can

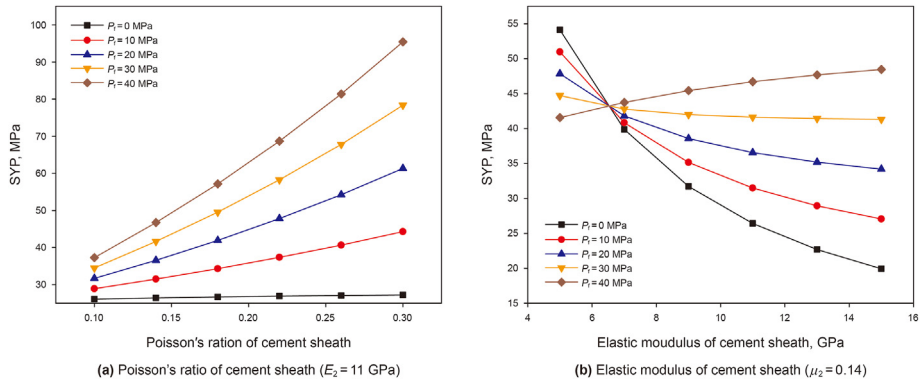

(a) Poisson's ratio of cement sheath (E_2 = 11 GPa) **(b)** Elastic modulus of cement sheath (μ_2 = 0.14)

Fig. 16. SYP under different formation stress.

Table 2
Matching between mechanical parameters of cement sheath and casing pressures.

P_c, MPa	P_f, MPa	μ_2, Dimensionless	E_2, GPa	T_{min}, MPa	*UCS*, MPa	T_0, MPa
40	0	≥0.10	≤7.5	>1.58	42.63	5.82
50	0	≥0.10	≤5.0	>1.98	20.70	2.54
60	0	≥0.22	≤5.0	>2.16	20.70	2.54
70	0	≥0.26	≤5.0	>2.47	20.70	2.54
70	10	≥0.28	≤7.0	>1.54	27.85	3.61
70	20	≥0.26	≤9.0	>0.57	35.28	4.73
70	30	≥0.24	≤11.0	>0.31	43.01	5.88
70	40	≥0.22	≥5.0	>0.14	20.70	2.54

T_{min}-the minimum tensile strength of cement sheath required under certain working conditions.

be ignored. For the failure of cement sheath integrity, the priority is that the cement sheath does not enter the plastic state, and the second is that interface debonding and tensile failure of cement sheath should be avoided as much as possible. Combining with Andrade (De Andrade and Sangesland, 2016b), the statistical relationship of compressive strength, tensile strength and elastic modulus under different cement slurry systems after hardening were used to establish the matching relationship between mechanical parameters of cement sheath and CSF system, as shown in Eq. (32) and Eq. (33). (De Andrade and Sangesland, 2016b).

$$UCS = 0.0354E_{cem}^2 + 3.1509E_{cem} + 4.0642 \tag{32}$$

$$T_0 = 0.1502UCS - 0.5732 \tag{33}$$

where E_{cem} is the elastic modulus of cement sheath; *UCS* is the compressive strength of cement sheath; T_0 is the tensile strength of cement sheath.

The mechanical parameters of cement sheath are calculated based on the criterion that the cement sheath does not enter plasticity. The results are shown in Table 2. It can be seen that with the increase of casing pressure, the performance requirements of cement sheath are higher, but even under 70 MPa, the tensile strength of cement sheath obtained according to Andrade's statistical relationship can still meet the requirements of this working condition. The cement sheath integrity at different well depths have different requirements on mechanical parameters of cement sheath, especially when P_f = 40 MPa, it shows a reverse state. When the elastic modulus of cement sheath is 5 GPa and Poisson's ratio is 0.26, the cement sheath integrity will not be damaged.

5. Conclusion

(1) An elastic-plastic mechanical model of casing-cement sheath-formation system is established with due consideration of the matching relationship between mechanical parameters and integrity of casing-cement sheath-formation system, by which the failure mechanism of cement sheath under alternating pressure is revealed. And the matching relationship between mechanical parameters of cement sheath and casing-cement sheath-formation system is obtained in the whole well section.

(2) The formation of interface debonding (casing-cement sheath interface and cement sheath-formation interface) is mainly related to the plastic strain accumulation, and there is a risk of micro-annulus at interface under alternating pressure, once the cement sheath enters plasticity whether in shallow or deep well sections.

(3) It has been found that there is a “critical range” in the Poisson's ratio of cement sheath. When the Poisson's ratio of cement sheath is higher than the “critical range”, the yield internal pressure of cement sheath decreases with the increase of the elastic modulus. At this time, reducing the elastic modulus can effectively improve the yield internal pressure of cement sheath. When the Poisson's ratio of cement sheath is lower than the “critical range”, the yield internal pressure of cement sheath increases with the increase of elastic modulus. At this time, increasing the elastic modulus can increase the yield internal pressure of cement sheath. When the Poisson's ratio of cement sheath is near the “critical range”, the yield internal pressure of cement sheath has little change with its elastic modulus. At this time, changing the elastic modulus has little effect on the yield internal pressure of cement sheath.

(4) It has been found that the matching relationship between mechanical parameters of cement sheath and casing-cement sheath-formation system is particularly important to the cement sheath integrity under alternating pressure, which provides a new method and concept for the optimization design of wellbore integrity and cement sheath integrity.

6. Discussion

Combining Section 3 and Section 4, the reasonable matching of elastic modulus and Poisson's ratio of cement sheath can effectively prevent the integrity failure of cement sheath. At present, toughening materials (Fiber, Latex, Expansion toughening) are added to

cement slurry to decrease the elastic modulus of cement sheath. The Poisson's ratio of cement sheath can be changed by adding some hard materials (Carbon nanotubes, Steel fibers, Basalt). However, the elastic modulus of cement sheath cannot be indefinitely decreased, and the Poisson's ratio of cement sheath cannot be indefinitely increased. The reasonable matching relationship between the elastic modulus and Poisson's ratio of cement sheath provides a new idea for the research and development of new cement slurry system.

Declaration of competing interest

The authors declared that they have no conflicts of interest to this work. We declare that we do not have any commercial or associative interest that represents a conflict of interest in connection with the work submitted.

Acknowledgments

Research work was financed by the National Natural Science Foundation of China (No. 52074232) and Sichuan Science and Technology Program (No. 2022NSFSC0028, No.2022NSFSC0994). Without their support, this work would not have been possible.

References

Agzamov, F., Ismagilova, E., 2019. Self-healing cements - the key to maintaining the integrity of cement sheath. Part 1. Nanotechnologies in Construction 11 (5), 577–586. https://doi.org/10.15828/2075-8545-2019-11-5-577-586.

Boukhelifa, L., Moroni, N., James, S.G., et al., 2005. Evaluation of cement systems for oil and gas-well zonal isolation in a full-scale annular geometry. SPE Drill. Complet. 20 (1), 44–53. https://doi.org/10.2118/87195-pa.

Bu, Y., Yu, L., Guo, S., et al., 2016. The cement sheath stress distribution research in shallow formation of the deep water area. Sci. Technol. Eng. 16 (26), 155–160. CNKI:SUN:KXJS.10.2016-23-029 (in Chinese).

Chen, H., Salip, A.F., 2004. Elasticity and Plasticity. China Architecture & Building Press, Beijing.

Chen, J., 2017. Mechanical Deformation Regular Pattern of Cement Ring and its Influence on Structural Integrity. Northeast Petroleum University.

Chen, Z., Cai, Y., 2009. Study on casing load in a casing-formation system by elastoplastic theory. Petrol. Explor. Dev. 36 (2), 242–246. https://doi.org/10.3321/j.issn:1000-0747.2009.02.017.

Chu, W., Shen, J., Yang, Y., et al., 2015. Calculation of micro-annulus size in casing-cement sheath-formation system under continuous internal casing pressure change. Petrol. Explor. Dev. 42 (3), 414–421. https://doi.org/10.11698/PED.2015.03.16.

Contreras, E., Johnson, K., Rasner, D., et al., 2019. Engineered vesicles for the controlled release of chemical additives and application for enhanced oil well cement integrity. In: SPE International Conference on Oilfield Chemistry, 8–9 April. Galveston, Texas. https://doi.org/10.2118/193538-MS.

De Andrade, J., Sangesland, S., Skorpa, R., et al., 2016. Experimental laboratory setup for visualization and quantification of cement-sheath integrity. SPE Drill. Complet. 31 (4), 317–326. https://doi.org/10.2118/173871-Pa.

De Andrade, J., Sangesland, S., 2016. Cement sheath failure mechanisms: numerical estimates to design for long-term well integrity. J. Petrol. Sci. Eng. 147, 682–698. https://doi.org/10.1016/j.petrol.2016.08.032.

De Andrade, J., Sangesland, S., Todorovic, J., et al., 2015. Cement sheath integrity during thermal cycling: a novel approach for experimental tests of cement systems. SPE Bergen One Day Seminar, 22 April, Bergen, Norway. https://doi.org/10.2118/173871-MS.

Deng, K., Lin, Y., Yi, H., et al., 2020. Experimental study on the integrity of casing-cement sheath in shale gas wells under pressure and temperature cycle loading. J. Petrol. Sci. Eng. 195, 107548. https://doi.org/10.1016/j.petrol.2020.107548.

Du, A., 2016. Study on Wellbore Integrity of Gas Storage in Depleted Oil and Gas Reservoir. Southwest Petroleum University.

Fan, M., Liu, G., Li, J., et al., 2016. Micro-gap generation mechanism on cement sheath interface under alternating thermal stress. Sci. Technol. Eng. 16 (19), 72–83. CNKI:SUN:KXJS.10.2016-19-011 (in Chinese).

Fan, M., Li, S., Li, J., et al., 2019. Numerical simulation of interface seal failure of cement sheath during multi-stage fracturing. Sci. Technol. Eng. 19 (24), 107–112. CNKI:SUN:KXJS.10.2019-24-020 (in Chinese).

Goodwin, K.J., Crook, R.J., 1992. Cement sheath stress failure. SPE Drill. Eng. 7 (4), 291–296. https://doi.org/10.2118/20453-pa.

Guan, Z., Liao, H., Lin, Z., et al., 2021. Test device for evaluating cement sheath seal integrity under cyclic loading. China Petroleum Machinery 49 (5), 48–53. https://doi.org/10.16082/j.cnki.issn.1001-4578.2021.05.007 (in Chinese).

Guo, X., Wu, Y., Bu, Y., et al., 2018. Elastoplastic analysis of wellbore integrity under varying internal casing pressure. J. China Univ.Petroleum 42 (3), 64–69. CNKI:SUN:SYDX.10.2018-03-008 (in Chinese).

Jackson, P.B., Murphey, C.E., 1993. Effect of Casing Pressure on Gas Flow through a Sheath of Set Cement. SPE/IADC Drilling Conference, 22–25 February, Amsterdam, Netherlands. https://doi.org/10.2118/25698-MS.

Lamik, A., Pittino, G., Prohaska-Marchried, M., 2021. Evaluation of cement-casing & cement-rock bond integrity during well operations. In: SPE/IADC Middle East Drilling Technology Conference and Exhibition, 25–27 May. https://doi.org/10.2118/202186-MS. Abu Dhabi, UAE.

Li, J., Chen, M., Liu, G., et al., 2005a. Elastic-plastic analysis of casing-concrete sheath-rock combination. Acta Pet. Sin. 26 (6), 99–103. https://doi.org/10.3321/j.issn:0253-2697.2005.06.023 (in Chinese).

Li, J., Chen, M., Zhang, H., et al., 2005b. Effects of cement sheath elastic modulus on casing external collapse load. J. China Univ. Pet. 29 (6), 41–44. https://doi.org/10.3321/j.issn:1000-5870.2005.06.010 (in Chinese).

Li, X., Zeng, Y., Muchiri, N., et al., 2022. The use of distributed acoustic sensing (DAS) in monitoring the integrity of cement-casing system. J. Petrol. Sci. Eng. 208, 10960. https://doi.org/10.1016/j.petrol.2021.109690.

Li, T., Guan, Z., Li, J., et al., 2019. Matching relationship between casing-cement sheath-stratum in gas storages. Transp. Storage 38 (11), 1265–1270. https://doi.org/10.6047/j.issn.1000-8241.2019.11.010 (in Chinese).

Lin, Y., Deng, K., Yi, H., et al., 2020. Integrity tests of cement sheath for shale gas wells under strong alternating thermal loads. Nat. Gas. Ind. 40 (5), 81–88. https://doi.org/10.3787/j.issn.1000-0976.2020.05.010 (in Chinese).

Liu, K., Ding, S.D., Zhou, S.M., et al., 2021. Study on preapplied annulus backpressure increasing the sealing ability of cement sheath in shale gas wells. SPE J. 26 (6), 3544–3560. https://doi.org/10.2118/205360-Pa.

Liu, K., Gao, D.L., Taleghani, A.D., 2018. Analysis on integrity of cement sheath in the vertical section of wells during hydraulic fracturing. J. Petrol. Sci. Eng. 168, 370–379. https://doi.org/10.1016/j.petrol.2018.05.016.

Liu, K., Wang, Y., Gao, D., et al., 2016a. Effects of hydraulic fracturing on horizontal wellbore for shale gas. Acta Pet. Sin. 37 (3), 406–414. https://doi.org/10.7623/syxb201603013 (in Chinese).

Liu, R., Zhang, L., Tao, Q., et al., 2016b. Experimental study on airtightness of cement sheath under alternating stress. Drill. Fluid Complet. Fluid 33 (4), 74–78. https://doi.org/10.3696/j.issn.1001-5620.2016.04.015 (in Chinese).

Meng, M., Frash, L., Carey, J.W., et al., 2021. Predicting cement-sheath integrity with consideration of initial state of stress and thermoporoelastic effects. SPE J. 26 (6), 3505–3528. https://doi.org/10.2118/205344-Pa.

Mueller, D.T., GoBoncan, V., Dillenbeck, R.L., et al., 2004. Characterizing Casing-Cement-Formation Interactions under Stress Conditions: Impact on Long-Term Zonal Isolation, 26–29 September. SPE Annual Technical Conference and Exhibition, Houston, Texas. https://doi.org/10.2118/90450-MS.

Shen, J., Shi, L., Li, Y., et al., 2017. Analysis and perspective of cement sheath integrity under a high differential pressure. Nat. Gas. Ind. 37 (4), 98–108. https://doi.org/10.3787/j.issn.1000-0976.2017.04.012 (in Chinese).

Tao, Q., 2018. Long-time sealing failure mechanism of cement sheath in gas wells and preventive measures. Drill. Prod. Technol. 41 (3), 25–28.. CNKI:SUN:ZCGY.10.2018-03-008 (in Chinese).

Therond, E., Bois, A.P., Whaley, K., et al., 2017. Large-scale testing and modeling for cement zonal isolation in water-injection wells. SPE Drill. Complet. 32 (4), 290–300. https://doi.org/10.2118/181428-Pa.

Thiercelin, M.J., Dargaud, B., Baret, J.F., et al., 1998. Cement design based on cement mechanical response. SPE Drill. Complet. 13 (4), 266–273. https://doi.org/10.2118/52890-pa.

Wang, L., Yang, C., Guo, Y., et al., 2019. Experimental and numerical investigation on the cement sheath sealing failure induced by large-scale multistage hydraulic fracturing in shale gas well. In: 53rd U.S. Rock Mechanics/Geomechanics Symposium, 23–26 June (New York City, New York).

Wang, Y., Li, J., Yang, X., et al., 2008. Research on matching cement's elastic modulus and Poisson's ratio with formation lithology. Petroleum Drilling Tech. 36 (6), 25–29. https://doi.org/10.3969/j.issn.1001-0890.2008.06.006.

Xi, Y., Li, J., Tao, Q., et al., 2020a. Experimental and numerical investigations of accumulated plastic deformation in cement sheath during multistage fracturing in shale gas wells. J. Petrol. Sci. Eng. 187, 106790. ARTN106790.10.1016/j.petrol.2019.106790.

Xi, Y., Li, J., Tao, Q., et al., 2020b. Emergence and evolution of micro-annulus under cyclic loading. Fault-Block Oil Gas Field 27 (4), 522–527. https://doi.org/10.6056/dkyqt202004024 (in Chinese).

Xu, H., Zhang, Z., Xiong, J., 2014. Influence of free casing on the stress and integrity of cement sheath in HTHP gas wells. Drill. Prod. Technol. 37 (2), 75–78. https://doi.org/10.3969/J.ISSN.1006-768X.2014.02.22.

Yan, W., Zou, L.Z., Li, H., et al., 2017. Investigation of casing deformation during hydraulic fracturing in high geo-stress shale gas play. J. Petrol. Sci. Eng. 150, 22–29. https://doi.org/10.1016/j.petrol.2016.11.007.

Yang, Y., Fang, Z., Yuan, B., et al., 2021. Integrity evaluation of the first interface of cement sheath based on tensile bonding strength. J. Southwest Pet. Univ. (Sci. & Technol. Edition) 43 (4), 183–190. https://doi.org/10.11885/j.issn.1674-5086.2021.04.29.13 (in Chinese).

Yin, Y., Cai, Y., Chen, Z., et al., 2006. Theoretical solution of casing loading in non-uniform ground stress field. Acta Pet. Sin. 27 (4), 133–138. https://doi.org/10.3321/j.issn:0253-2697.2006.04.030 (in Chinese).

Zeng, Y., Liu, R., Li, X., et al., 2019. Cement sheath sealing integrity evaluation under cyclic loading using large-scale sealing evaluation equipment for complex

subsurface settings. J. Petrol. Sci. Eng. 176, 811–820. https://doi.org/10.1016/j.petrol.2019.02.014.
Zhang, H., Shen, R.C., Yuan, G.J., et al., 2017. Cement sheath integrity analysis of underground gas storage well based on elastoplastic theory. J. Petrol. Sci. Eng. 159, 818–829. https://doi.org/10.1016/j.petrol.2017.10.012.
Zhou, S., Liu, R., Zeng, H., et al., 2019. Mechanical characteristics of well cement under cyclic loading and its influence on the integrity of shale gas wellbores. Fuel 250, 132–143. https://doi.org/10.1016/j.fuel.2019.03.131.
Zhao, X., Guan, Z., Liao, H., et al., 2015. Study on cementing micro-annulus at interface generation rules under alternating casing pressure. China Petroleum Machinery 43 (4), 22–27. https://doi.org/10.3969/j.issn.1673-5005.2014.04.012 (in Chinese).
Zhang, X., Wang, L., Bi, Z., et al., 2022a. Mechanical analysis on cement sheath integrity under asymmetric load. J. Pet. Explor. Prod. Technol. 12 (1), 135–146. https://doi.org/10.1007/s13202-021-01346-4.
Zhang, X., Bi, Z., Wang, L., et al., 2022b. Shakedown analysis on the integrity of cement sheath under deep and large-scale multi-section hydraulic fracturing. J. Petrol. Sci. Eng. 208, 109619. https://doi.org/10.1016/j.petrol. 2021.109619.